

BeppoSAX confirms extreme relativistic effects in the X-ray spectrum of MCG-6-30-15

M. Guainazzi¹, G. Matt², S. Molendi³, A. Orr¹, F. Fiore^{4,5}, P. Grandi⁶, A. Matteuzzi⁵, T. Mineo⁷, G.C. Perola², A.N. Parmar¹, L. Piro⁶

¹ Astrophysics Division, Space Science Department of ESA, ESTEC, Postbus 299, NL-2200 AG Noordwijk, The Netherlands

² Dipartimento di Fisica “E. Amaldi”, Università degli Studi “Roma Tre”, Via della Vasca Navale 84, I-00146 Roma, Italy

³ Istituto di Fisica Cosmica “G. Occhialini”, CNR, Via Bassini 15, I-20133 Milano, Italy

⁴ Osservatorio Astronomico di Roma, Via dell’Osservatorio, I-00144 Monteporzio Catone, Italy

⁵ BeppoSAX Science Data Center, Via Corolle 19, I-00131 Roma, Italy

⁶ Istituto di Astrofisica Spaziale CNR, Via Fosso del Cavaliere, I-00133 Roma, Italy

⁷ Istituto di Fisica Cosmica ed Applicazioni dell’Informatica CNR, Via Ugo La Malfa 153, I-90146 Palermo, Italy

Received; accepted

Abstract. We report in this *Letter* the first simultaneous measure of the X-ray broadband (0.1–200 keV) continuum and of the iron K_{α} fluorescent line profile in the Seyfert 1 galaxy MCG-6-30-15. Our data confirms the ASCA detection of a skewed and redshifted line profile (Tanaka et al. 1995). The most straightforward explanation is that the line photons are emitted in the innermost regions of a X-ray illuminated relativistic disk. The line Equivalent Width ($\simeq 200$ eV) is perfectly consistent with the expected value for solar abundances, given the observed amount of Compton reflection. We report also the discovery of a cut-off in the nuclear primary emission at the energy of $\simeq 160$ keV.

Key words: Accretion disks – Line: formation – Line: profiles – Galaxies: individual: MCG-6-30-15 – Galaxies: Seyfert – X-rays: general

1. Introduction

There is general consensus on the idea that the energy output of Active Galactic Nuclei (AGN) is due to the release of radiation by matter falling onto a supermassive black hole. Evidence of the presence of such a black hole was only indirect before the launch of the X-ray satellite ASCA. A long-look observation of the Seyfert 1 galaxy MCG-6-30-15 revealed that the profile of the K_{α} iron fluorescent line is broad, skewed and double-horned (Tanaka et al. 1995). These are the expected signatures of kinematics and relativistic effects when photons are emitted in the innermost regions of a X-ray illuminated accretion disk (Fabian et al. 1989; Matt et al. 1992). Alternative explanations for the observed line turn out to be unplausible (Fabian et al.

1995). The iron line is generally broad in the Seyfert 1s observed by ASCA (Mushotzky et al. 1995; Guainazzi et al. 1997; Nandra et al. 1997). However, the limited ASCA energy bandpass did not allow a precise determination of the underlying continuum, and - in particular - of the reflection component. Usually, reflection from an infinite, plane-parallel slab was assumed, following the findings of the X-ray satellite Ginga (Nandra & Pounds 1994). This can in principle affect significantly the measurement of the iron line profile, as shown by Cappi et al. (1996).

The scientific payload onboard BeppoSAX (Boella et al. 1997a) covers for the first time simultaneously the broad energy band between 0.1 and 200 keV. It is therefore particularly suited to properly deconvolve complex spectra. Although the energy resolution of the BeppoSAX detectors is worse than that of ASCA CCD’s ($\simeq 8\%$ versus $\simeq 2\%$ at 6 keV), the better estimate of the underlying continuum can provide complementary information on the broad iron lines. In this *Letter* we report on the BeppoSAX study of the iron line in MCG-6-30-15, which is both the best case for a relativistic line in ASCA data and one of the Seyfert 1s observed by BeppoSAX with a long exposure time (~ 160 ks). In the following we will focus on the high energy, time-average spectrum. The soft X-ray spectrum is described in detail by Orr et al. (1997).

2. Observation and data preparation

MCG-6-30-15 was observed by BeppoSAX from 1996 July 29, 18:49:48 UT to August 3 03:15:00. Data reduction and analysis follow the guidelines in Matt et al. (1997). Only data from the Low Energy Concentrator Spectrometer (LECS, 0.1–4 keV; Parmar et al. 1997), the Medium Energy Concentrator Spectrometer (MECS; 1.8–10.5 keV; Boella et al. 1997b) and the Phoswitch Detector System (PDS; 13–200 keV; Frontera et al. 1997) are discussed. To-

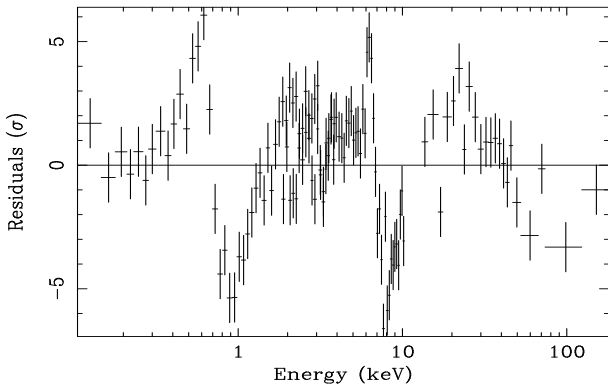


Fig. 1. Residuals in units of standard deviation when a photoelectric absorbed power-law is applied to the LECS, MECS and PDS data

tal exposure times were about 42 ks, 164 ks, and 86 ks for the LECS, MECS and PDS, respectively. Spectra of the imaging instruments have been extracted from circular regions of radius 8' around the centroid of the source. Total net count rates were $0.474 \pm 0.003 \text{ s}^{-1}$, $0.966 \pm 0.002 \text{ s}^{-1}$ and $0.70 \pm 0.03 \text{ s}^{-1}$ in the LECS, MECS and PDS, respectively.

In this *Letter*: errors are quoted at 90% level of confidence for each parameter ($\Delta\chi^2 = 2.71$, Lampton, Margon & Bowyer 1976); energies are in the source rest frame.

3. Results

We have fitted the spectra of all detectors simultaneously. In Fig. 1 the residuals are shown, when a simple absorbed power law is applied. The spectral complexity is apparent: an edge-like feature at $\simeq 0.7$ keV is the imprinting of warm absorbing matter along the line of sight (Nandra & Pounds 1992; Fabian et al. 1994); an emission line, peaking at $\simeq 6.3$ keV, is broadly consistent with K_{α} fluorescence from neutral or mildly ionized iron; a continuum “bump”, peaking at $\simeq 20$ keV, is associated with Compton scattering of the primary continuum by optically thick matter surrounding the central black hole. The last two ingredients are known to be ubiquitously present in the X-ray spectra of Seyfert 1 galaxies (Nandra & Pounds 1994; Matt 1998).

We have assumed therefore a “baseline” model composed by: a power-law, a Compton-reflection component (model `pexrav` in XSPEC, Magdziarz & Zdziarski 1995) with the inclination angle held fixed to 35° (see later) and a “warm absorber”. Following Orr et al. (1997), the warm absorber has been parameterized as a set of four absorption edges, with threshold energies fixed at those expected from the following ionized species: O⁷⁺, O⁸⁺, Ne⁸⁺, Ne⁹⁺. However, we were forced to add several further component to this parameterization, in order to achieve a robust estimate of the intrinsic power-law and a χ^2 reasonably close to one, and namely: a) a narrow emission line

with centroid energy $E_C = 0.62 \pm 0.03$ keV and Equivalent Width $EW = 33 \pm 15$ eV; b) a narrow emission line with $E_C = 0.86 \pm 0.03$ keV and $EW = 60 \pm 40$ eV; c) an absorption edge with threshold energy $E_{th} = 7.6 \pm 0.2$ keV and optical depth $\tau = 0.14 \pm 0.05$. These features are likely to be associated with the ionized absorber; they are consistent with K_{α} O⁷⁺, iron-L (or K_{α} Ne⁸⁺–⁹⁺) fluorescence transitions, and photoabsorption from Fe^{5+–7+}, respectively. A detailed discussion of these features is beyond the focus of this *Letter*. Similar results on the high-energy continuum and iron line as those presented later are obtained if the self-consistent warm absorber model `absori` in XSPEC is used.

In Fig. 2, the residuals are shown when the “baseline” model is applied to the whole energy range, but excluding the 4–7.5 keV interval, where the relativistic iron line is expected to be present. The iron line profile is *remarkably similar to that of ASCA* (cf. Fig. 1 in Tanaka et al. 1995). This is the first independent confirmation of the existence of extreme relativistic effects in the X-ray spectrum of MCG-6-30-15. This result is of particular importance because of the more reliable continuum determination provided by BeppoSAX.

Several descriptions of the line profile have been tried, whose best-fit parameters are listed in Table 1. A simple Gaussian profile leaves significant residuals in the 4–5 keV energy band (see Fig. 3), which justify the addition of a second broad line. If we assume that the first line is narrow and “neutral” (i.e.: centroid held fixed at 6.4 keV), $\Delta\chi^2$ is equal to 13.7 for 1 further degree of freedom, significant at more than 99.9% level. However, there is no straightforward physical explanations for a broad line with $E_C \simeq 4.5$ keV outside the relativistic scenario. We have then tried models of relativistic line profiles around a Schwarzschild (`diskline` in XSPEC, Fabian et al. 1989) or a Kerr (`laor` in XSPEC, Laor 1991) black hole. In both these models the internal radius of the emitting region has been held fixed to the last stable orbit (6 and 1.23 gravitational radii r_g , respectively) and the emissivity radial function parameterized as r^{-2} (the results are marginally affected by any choice of the emissivity index in the range -2 to -3). The addition of a further narrow Gaussian line to the relativistic models yields a negligible change in the χ^2 and the 90% upper limit on its EW is 40 eV. All the above models yield acceptable fits at 90% level. However, even the best relativistic model is still not capable to fully account for the redmost tail of the profile (see Fig. 3). Iwasawa et al. (1996) have shown that the contrast between the blue horn and the red tail diminishes in very low intensity states. MCG-6-30-15 exhibited variability by a factor of four on timescales as low as a few thousands seconds during the BeppoSAX observation (Orr et al. 1997). It is then likely that the true line profile is a superposition of different states and is then still different from the steady state template. Common features of both the relativistic models are an EW of the order of

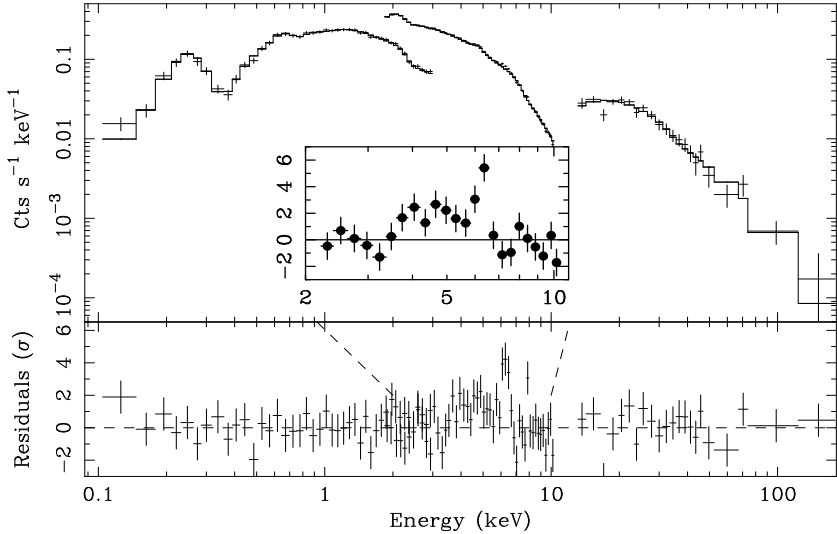


Fig. 2. Spectra (*upper panel*) and residuals in units of standard deviation (*lower panel*) when the best-fit baseline continuum is applied on the whole band except the 4–7.5 keV energy range (details in text). In the *inset*, the MECS residuals only, binned by a further factor of 2. The best-fit parameters for such a continuum are: $\Gamma = 2.00$, $R = 1.2$ and $E_{\text{cutoff}} = 130$ keV

Table 1. Best-fit results and parameters when the “baseline” continuum is applied and the iron line modeled as in Column 1.

Model	N_{H} (10^{20} cm^{-2})	Γ	R	E_{cutoff} (keV)	E_{C} or R_o (keV) or (r_g)	σ or i (keV) or $^{\circ}$	EW (keV)	χ^2
Single Gaussian	6.3 ± 0.3	1.97 ± 0.05	1.0 ± 0.3	110 ± 30	6.37 ± 0.09	< 0.18	50 ± 15	144.3/124
Double Gaussian [†]	6.7 ± 0.4	2.04 ± 0.06	1.3 ± 0.4	130 ± 40	4.5 ± 0.8	0.8 ± 0.3	90 ± 40 and 70 ± 20 ^b	130.6/123
Schwarzschild	6.8 ± 0.3	2.06 ± 0.03	1.2 ± 0.4	160 ± 130	7.2 ± 2.6	36 ± 2	200 ± 60	138.0/124
Kerr	6.8 ± 0.2	2.068 ± 0.018	1.2 ± 0.2	150 ± 50	11 ± 5	34 ± 8	220 ± 70	145.7/124

[†]fixed

^ain this model, the second Gaussian line has $E_{\text{C}} = 6.4$ keV and $\sigma = 0$.

^bfor the broad and narrow components, respectively

200 eV, a rather small outer radius of the line emitting region ($R_o \lesssim 17$ gravitational radii, r_g) and an inclination angle $\simeq 35^{\circ}$. A worse fit is obtained in the Schwarzschild scenario ($\chi^2 = 145.2/124$ dof) if one assumes a large outer radius (*e.g.*: $R_o = 10^3 r_g$) and allows the inner radius to be free.

The best-fit broadband continuum parameters are in good agreement with the ones observed in MCG-6-30-15 by previous missions (Fiore et al. 1992). MCG-6-30-15 confirms to have a slightly steeper intrinsic continuum ($\Gamma \simeq 2.06$) than the average measured in Seyfert 1 as a class (Nandra et al. 1994; Nandra et al. 1997). The amount of reflection (parameterized thorough the relative normalization between the reflected and the primary components R) is consistent with that expected from an isotropically-illuminated, plane-parallel infinite slab. For the first time, a cutoff in the primary continuum has been measured in

MCG-6-30-15, with E_{cutoff} comprised in the range 100–400 keV at 90% confidence level for two interesting parameters (see Fig. 4). The average observed 2–10 keV flux is $5.4 \times 10^{-11} \text{ erg cm}^{-2} \text{ s}^{-1}$, corresponding to an unabsorbed rest frame luminosity of $1.50 \times 10^{43} \text{ erg s}^{-1}$ (we assume $H_0 = 50 \text{ km s}^{-1} \text{ Mpc}^{-1}$ and $z = 0.008$). It is about 60% higher than in the long-look ASCA observation (Tanaka et al. 1995).

4. Conclusions

The analysis of the BeppoSAX observation of the Seyfert 1 galaxy MCG-6-30-15 fully confirms the ASCA discovery of a relativistic iron line. The unprecedented broad bandwidth of BeppoSAX permitted a precise determination of the underlying continuum, thereby overcoming a potential criticisms to the ASCA result. The amount of reflection continuum is consistent with the one assumed by Tanaka

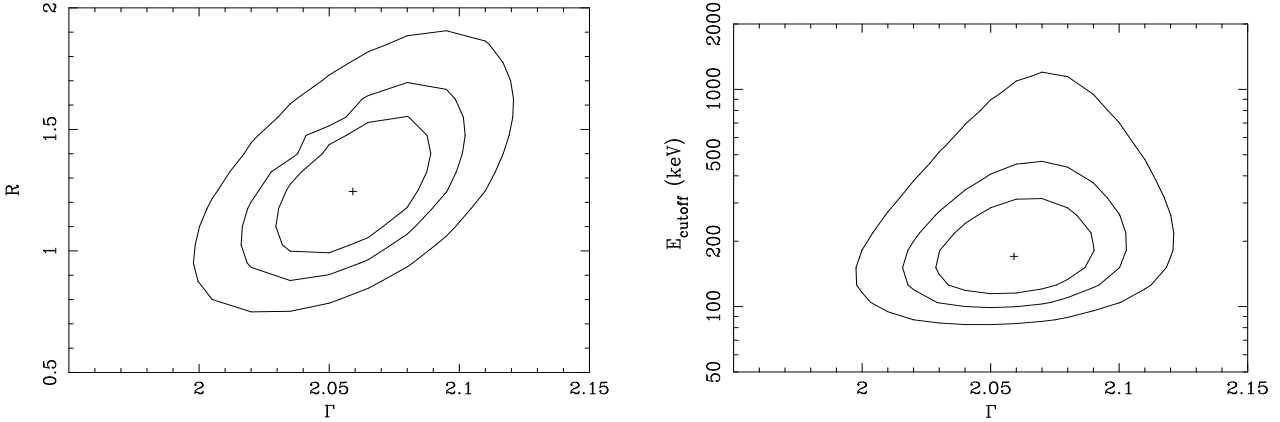


Fig. 4. *Left panel:* Γ vs. R contour plot for the baseline + Schwarzschild relativistic line profile model. *Right panel:* cutoff energy vs. Γ

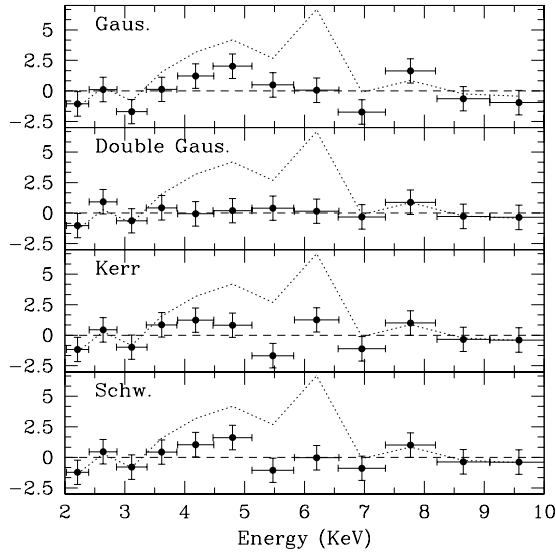


Fig. 3. MECS residuals in units of standard deviations when the following models are employed to fit the iron line profile (from top to bottom): single Gaussian, double Gaussian, Kerr relativistic profile, Schwarzschild relativistic profile. In all panels, the dotted line represents the envelope of the residuals in the inset of Fig. 2, to illustrate, for sake of comparison, the unfitted line profile against the underling continuum

et al. (1995). The bulk of the iron line is produced very close to the black hole and the system is seen at a moderate inclination angle, in agreement with ASCA findings. However, the EW ($\simeq 200$ eV) measured by BeppoSAX is consistent with the expected value for solar abundances, given the value of R (Matt et al. 1992). These data do not require any *ad hoc* iron overabundance, such as the

ASCA measurement of the same quantity ($\simeq 330$ eV) had suggested (Tanaka et al. 1995).

Acknowledgements. The BeppoSAX satellite is a joint Italian-Dutch program. MG and AO acknowledge the receipt of an ESA Research Fellowship. GM acknowledges financial support from ASI and MURST.

References

- Boella G., Perola G.C., Scarsi L., 1997a, A&AS 122, 299
- Boella G., Chiappetti L., Conti G., et al., 1997b, A&AS 122, 372
- Cappi M., Mihara T., Matsuoka M., et al., 1996, ApJ 456, 141
- Dickey J.M., Lockman F.J., 1990, ARA&A 28, 215
- Fabian A.C., Rees M.J., Stella L., White N.E., 1989, MNRAS 238, 729
- Fabian A.C., Kunieda H., Inoue S., et al., 1994, PASJ 46, 65
- Fabian A.C., Nandra K., Reynolds C.S., et al., 1995, MNRAS 277, 11
- Fiore F., Perola G.C., Matsuoka M., Yamauchi M., Piro L., 1992, A&A 262, 37
- Frontera F., Costa E., Dal Fiume D., et al., 1997, A&AS 122, 357
- Guainazzi M., Mihara T., Otani C., Matsuoka M., 1997, PASJ 48, 781
- Iwasawa K., Fabian A.C., Reynolds C.S., et al., 1996, MNRAS 282, 1038
- Lampton M., Margon B., Bowyer S., 1976, ApJ 208, 177
- Laor A., 1991, ApJ, 376, 90
- Magdziarz P., Zdziarski A.A., 1995, MNRAS 273, 837
- Matt G., Perola G.C., Piro L., Stella L., 1992, A&A 257, 63 (erratum 263, 453)
- Matt G., Guainazzi M., Frontera F., et al., 1997, A&A 325, L13
- Matt G., 1998, in Proceedings of the Conference “High Energy Processes in Accreting Black Holes”, Poutanen J. & Svensson R. eds., in press
- Mushotzky R.F., Fabian A.C., Iwasawa K., et al., 1995, MNRAS 272, 9
- Nandra K., Pounds K.A., 1992, Nat 359, 215
- Nandra K., Pounds K.A., 1994, MNRAS 268, 405

Nandra K., George I.M., Mushotzky R.F., Turner T.J., Yaqoob T., 1997, ApJ 477, 602
Orr A., Molendi S., Fiore F., et al., A&A 324, L77
Parmar A.N., Martin D.D.E., Baudzaz M., et al., 1997, A&AS 122, 309
Tanaka Y., Nandra K., Fabian A.C., et al., 1995, Nat 375, 659